
Temperature-Dependent Electrical Properties of p-Si/n-TiO₂ Thin Film Heterojunction Diodes Grown by Sol-Gel and E-Beam Evaporation Methods

3.1 Introduction

We have discussed in Chapter-2 that p-Si/n-TiO₂ thin film (TF) heterojunction diodes grown by EBE and SG deposition methods can be explored for ultraviolet detection and various sensing applications [Zhang *et al.* (2012-c)]. As discussed in Chapter-1, the I-V characteristics of the heterojunction diodes can be modelled by thermionic emission model commonly applied for the I-V characteristics modelling of the Schottky junctions [Sze (1981), Brillson and Lu (2011)]. Thus, it is quite obvious that the electrical parameters such as barrier height, ideality factor and reverse saturation current of the p-Si/n-TiO₂ heterojunction diodes considered in Chapter-2 must be temperature-dependent in the similar manner as analyzed in terms of barrier inhomogeneity phenomenon for the Schottky junction diodes by many researchers [Werner and Güttler (1991), Mtangi *et al.* (2009), Chirakkara *et al.* (2012), Ylmaz *et al.* (2012), Somvanshi and Jit (2013), Dias *et al.* (2014), Somvanshi and Jit (2014), Hazra and Jit (2014-b), Pillai *et al.* (2014), Yadav *et al.* (2014), Mayimele *et al.* (2015)]. The Barrier Height Inhomogeneity (BHI) phenomenon is referred to the temperature-dependent characteristics of the barrier height and ideality factor of a Schottky or heterojunction diode due to the non-ideal Schottky metal-semiconductor or heterojunction interface owing to interface states and other non-ideal interface characteristics. In order to include

the BHI phenomenon, the thermionic model based I-V characteristics of the Schottky or heterojunction diodes are modified by assuming a Gaussian distributed barrier height across the Schottky or heterojunction interface as suggested by Werner and Güttler [Werner and Güttler (1991)]. We have discussed in Chapter-1 that the method proposed by Werner and Güttler [Werner and Güttler (1991)] is widely used for extracting the electrical parameters of Schottky and heterojunction diodes from their temperature-dependent I-V (I-V-T) characteristics [Yadav *et al.* (2014), Hazra and Jit (2014-b)]. Although, some studies have been reported on the analysis of temperature-dependent I-V (I-V-T) characteristics for n-TiO₂ TF based Schottky and heterojunction devices [Pakma *et al.* (2008-b), Altuntas *et al.* (2009), Kınacı *et al.* (2012), Aksoy and Caglar (2014)], to the best of our knowledge, no experimental study has been reported so far on the estimation of effective Richardson constant of the n-TiO₂ TFs from measured I-V-T characteristics of n-TiO₂/p-Si based heterojunction diodes. Thus, the present chapter has been devoted to study the temperature-dependent electrical characteristics of two types of p-Si/n-TiO₂ heterojunction diodes based on the EBE and SG n-TiO₂ TFs already considered in Chapter-2. The outline of the present chapter can be given as follows:

Section 3.2 provides the device fabrication and experimental details. Section 3.3 discusses various results with the extraction of various temperature-dependent electrical properties from the measured I-V-T characteristics of the two types of heterojunction diodes. The value of the effective Richardson Constant of the TiO₂ has also been determined in this section. Finally, Section 3.4 has been used for the summary and conclusion of the works carried out in the present chapter.

3.2 Device Fabrication and Experimental Details

The details of the fabrication steps as well as structural, optical and electrical characterization of p-Si/n-TiO₂ TF heterojunction diodes prepared by the EBE and SG methods have already been presented in Chapter-2. However, we will briefly discuss the fabrication details of p-Si/n-TiO₂ heterojunction diodes for the ease of understanding of the readers. The device fabrication details include the standard cleaning of p-type Si substrates using piranha-HF method. Then for preparing SG based devices, the SG solution of TiO₂ is prepared using titanium tetraisopropoxide (TTIP) as a precursor and isopropyl alcohol as a solvent. After aging the solution for 24 hours, it is filtered and then used for coating the n-TiO₂ layer (of thickness ~120 nm) on p-Si substrates using spin coater unit (TSE, SPM-150LC). On the other hand, the EBE method has been used to deposit the n-TiO₂ layer (of thickness ~120 nm) on p-Si substrates for fabricating EBE based devices. Both the SG and EBE based TiO₂ TFs deposited on the p-Si substrates are annealed in Ar gas atmosphere at pre-optimized temperature of ~550 °C for 20 minutes for improving the quality of the films. Ti/Al (70 nm/50 nm) metal dots of ~1 mm diameter are deposited on the EBE and SG derived annealed TiO₂ films for making ohmic cathode contacts by using the EBE method. The Ti/Al (50 nm/40 nm) ohmic contact is also grown on the reverse side of the p-Si substrate by EBE method for obtaining the anode contact of the heterojunction. Finally, the heterojunctions are processed for post-metal deposited heat treatment in Ar gas atmosphere at ~450 °C for 7 minutes for improving the contact electrodes.

Now we will directly refer to all the results of Chapter-2 for the related discussions in the present chapter without repeating them here. However, it may be noted that the I-V characteristics considered in Chapter-2 were measured only at room temperature. In the present chapter, I-V characteristics of two types of heterojunction diodes under study

are measured over a temperature range of ~303 K to ~453 K by using the semiconductor parameter analyzer. We have used an in-house measurement setup for measuring temperature-dependent I-V (I-V-T) characteristics under dark condition. The fabricated heterojunction device was placed on the top of a thermal chuck for changing the operating temperature of the device under study. The I-V-T characteristics have been measured with the help of electrical probing to connect the device to the semiconductor parameter analyzer. We have used a rounded thermal chuck to provide an ultra-high temperature uniformity on the contact area of the device to be studied. The schematic structure of the fabricated p-Si/n-TiO₂ heterojunction diodes under consideration is already shown in Figure 2.19 of Chapter-2.

3.3 Results and Discussion

3.3.1 Temperature Dependent Current-Voltage (I-V-T) Characteristics of Si/TiO₂ TF Heterojunction Diodes

In order to examine the temperature-dependent electrical parameters of p-Si/n-TiO₂ TF heterojunction diodes as fabricated in Chapter-2, we measure the Current-Voltage (I-V) characteristics at several operating temperatures ranging from ~303 K to ~453 K. The measured temperature-dependent I-V characteristics of both fabricated diodes have been shown in Figure 3.1 (a) and (b). To avoid the effect of series resistance on diode parameters we have considered low current regions for our study, where the measured I-V characteristics can be approximated by Eq. (3.1) as considered by other researchers [Hazra and Jit (2014-b), Somvanshi and Jit (2014)]. Thus the rectifying I-V characteristics of n-TiO₂/p-Si heterojunction diodes fabricated in previous chapter can be expressed by TE model as [Hazra and Jit (2014-b)]:

$$I = I_0 \left\{ \exp\left(\frac{qV}{\eta kT}\right) - 1 \right\} \quad (3.1)$$

where, V is the applied bias, q is electronic charge, T is operating temperature, and k is the Boltzmann's constant. $\eta(T)$ and $I_0(T)$ are temperature-dependent ideality factor and reverse-saturation current expressed as [Somvanshi and Jit (2013)]:

$$\ln(I) = \ln(I_0) + \left(\frac{qV}{\eta kT}\right) \quad (3.2)$$

$$I_0 = AA^*T^2 \exp\left(-\frac{q\phi_{B,eff}}{kT}\right) \quad (3.3)$$

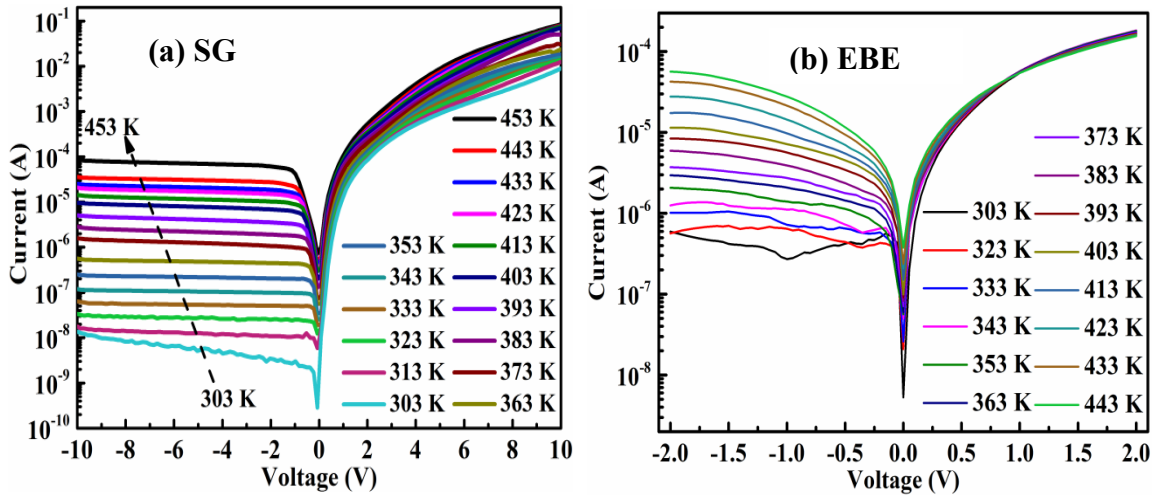


Figure 3.1: Measured temperature-dependent semi-logarithmic I-V characteristics over 303–453 K temperature range for the p-Si/n-TiO₂ heterojunction diodes fabricated by using (a) SG method (b) EBE method.

where, $A^* \sim 1200 \text{ Acm}^{-2}\text{K}^{-2}$ (for $m_n^* = 10m_o$) is the effective Richardson constant of TiO₂ [Zhang *et al.* (2012-a)], $A \sim 0.785 \times 10^{-2} \text{ cm}^2$ is the diode contact area, $\phi_{B,eff}$ is effective barrier height at zero bias which is expressed as [Somvanshi and Jit (2013)]:

$$\phi_{B,eff} = \left(\frac{kT}{q}\right) \ln\left(\frac{AA^*T^2}{I_0}\right) \quad (3.4)$$

$$\eta = \left(\frac{q}{kT} \right) \left\{ \frac{dV}{d(\ln I)} \right\} \quad (3.5)$$

For $V \gg kT/q$, Eq. (3.1) gives $I \approx I_0(T) \exp(qV/\eta kT)$ and $\ln(I)$ versus V plot gives a straight line whose intercept at $\ln(I)$ axis provides the value of $I_0(T)$ and slope can be used in Eq. (3.5) to determine η at a given temperature. Using the value of $I_0(T)$ in Eq. (3.4), we can compute $\phi_{B,eff}$. The estimated values of $I_0(T)$, η and $\phi_{B,eff}$ for the SG and EBE TiO₂ film based heterojunction diodes in the range of ~303 K to 354 K are tabulated in Table 3.1.

Table 3.1: Temperature-Dependent (I-V-T) Electrical Parameters of n-TiO₂/p-Si TF Heterojunction Diodes.

Temp. (K)	For SG Device			For EBE Device		
	η	$\Phi_{B,eff}$	$I_0(T)$	η	$\Phi_{B,eff}$	$I_0(T)$
303	3.3173	0.8638	4.3587E-9	3.1158	0.8107	2.9681E-8
313	3.2334	0.8833	5.7929E-9	-	-	-
323	2.9916	0.9105	6.3802E-9	2.7445	0.8602	3.8813E-8
333	2.9019	0.9346	7.8148E-9	2.6798	0.8812	5.0154E-8
343	2.82	0.9599	9.1073E-9	2.5832	0.8985	7.2572E-8
353	2.71611	0.9803	1.2383E-8	2.4669	0.9233	8.0447E-8
363	2.6832	0.9937	2.0727E-8	2.3931	0.9472	9.1282E-8
373	2.54682	1.0141	2.7139E-8	2.2275	0.9722	9.9899E-8
383	2.4993	1.0205	5.3638E-8	2.1022	0.9939	1.19861E-7
393	2.4376	1.0478	5.5442E-8	2.0523	1.0028	2.08899E-7
403	2.3838	1.0601	8.7906E-8	1.902	1.0209	2.7147E-7
413	2.3019	1.0742	1.3019E-7	1.7875	1.0379	3.60495E-7
423	2.2443	1.0926	1.6809E-7	1.7171	1.0545	4.7813E-7
433	2.2049	1.1119	2.0971E-7	1.6308	1.0728	5.97758E-7
443	2.1966	1.1296	2.702E-7	1.6035	1.0932	7.01758E-7
453	2.1251	1.1359	4.6175E-7	-	-	-

The results of Table 3.1 and Figure 3.1 show similar trends of variation of I_0 , η , and $\phi_{B,eff}$ with the change in temperature for both the heterojunctions under study. The

calculated values of ideality factors are in the range of ~ 3.1158 to ~ 1.6035 , and ~ 3.3173 to ~ 2.1251 for the EBE and SG based diodes, respectively. The lowest values of the ideality factor are found at the highest temperature. The SG based diode offers slightly larger value of the ideality factor than that of the EBE based device (see Figure 3.2). In both the devices under consideration η has been found deviating from its ideal value (where $\eta \approx 1$) as a consequence of non-ideal heterojunction interface of the device [Dias and Krupanidhia (2014)]. The estimated high values are attributed to several parameters such as series resistance and mismatching in the thermal expansion coefficient and lattice constants of Si and TiO₂. It may also be due to the strain developed in the TFs owing to high lattice mismatch or edge dislocation at the interfaces. The value of η approaches closer to the ideal value with the increase in temperature (see Figure 3.2) attributed to the increase in the carriers by thermionic emission process.

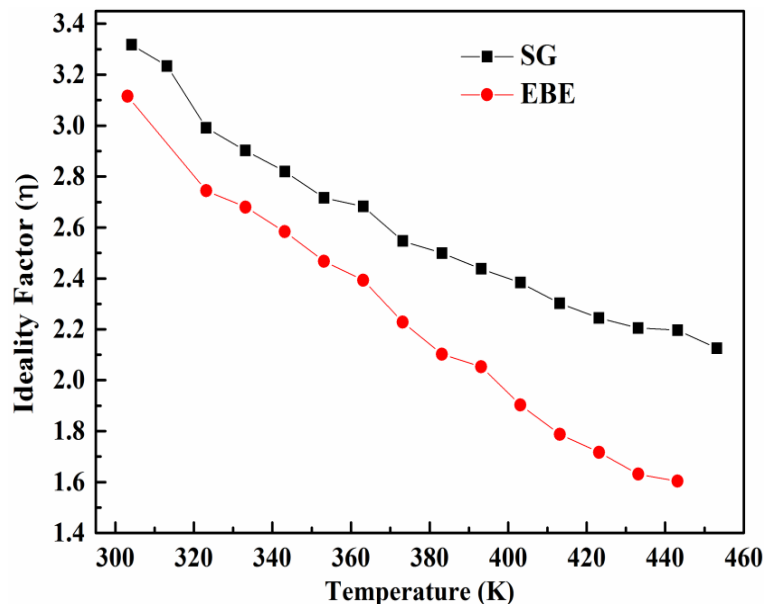


Figure 3.2: Variation of the ideality factor with temperature for both the devices fabricated using EBE and SG methods.

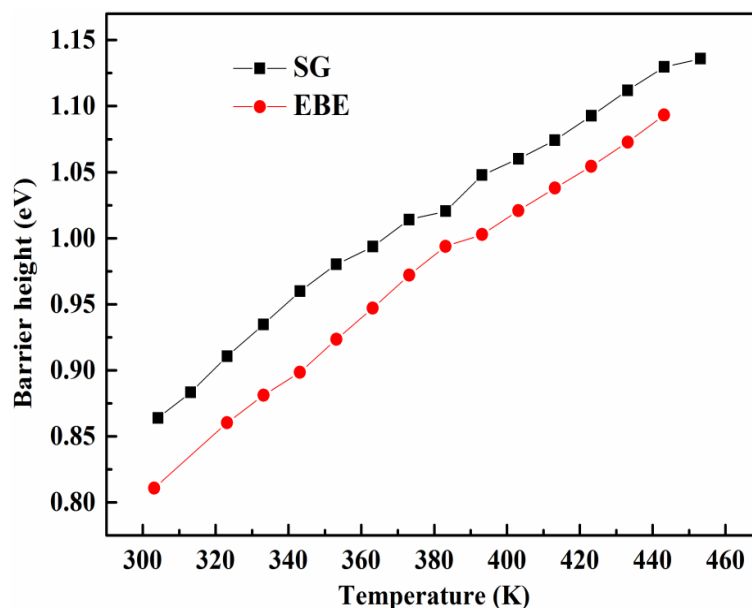


Figure 3.3: Variation of the barrier height with temperature for both the devices fabricated using EBE and SG methods.

The barrier height is observed to be increased with the temperature (see Figure 3.3) which is attributed to the presence of tunnelling, defects and Barrier Height Inhomogeneities (BHI) at the heterojunction interface [Majumdar and Banerjia (2009)]. The temperature-dependence of semiconductor band gap also explains the variation of measured barrier height. Several other researchers working on metal oxides based materials have reported similar behaviour which highlights the negative-temperature-coefficient of such devices [Mtangi *et al.* (2009), Altuntas *et al.* (2009), Chirakkara and Krupanidhi (2012)]. The barrier height of EBE based heterojunction diode is increased from ~ 0.8107 to ~ 1.0932 eV whereas it is changed from ~ 0.8638 to ~ 1.1359 eV for SG based heterojunction diode as shown in Figure 3.3. The observed behaviour is explained on the basis of temperature activated current transport phenomena [Sze (1981), Majumdar and Banerji (2009)]. From Figure 3.4 and Table 3.1, the reverse saturation current (I_0) is observed to be increased with the rise in temperature for both the devices. The value of I_0 is increased from $\sim 2.9681 \times 10^{-8}$ A (303 K) to $\sim 7.01758 \times 10^{-7}$ A (443 K)

for the EBE based heterojunction while it is increased from $\sim 4.3587 \times 10^{-9}$ A (303 K) to $\sim 4.6175 \times 10^{-7}$ A (453 K) for the SG based diode. The temperature-dependent barrier height and ideality factor characteristics can be explained in terms of the non-uniform spatial barrier distribution across the heterojunction interface due to non-ideal heterojunction interface originally proposed by Werner and Gütler [Werner and Gütler (1991)] for the Schottky diodes. The non-uniform distribution of the barrier height is known as the Barrier Height Inhomogeneity (BHI) phenomenon [Werner and Gütler (1991)]. Dominant factors affecting hetero-interface quality include the deposition methods, surface treatment (cleaning, plasma, etching, etc.), and surface defect density. The BHI at the interface is responsible for the apparent rise in the barrier height with increased temperature [Yılmaz *et al.* (2012)].

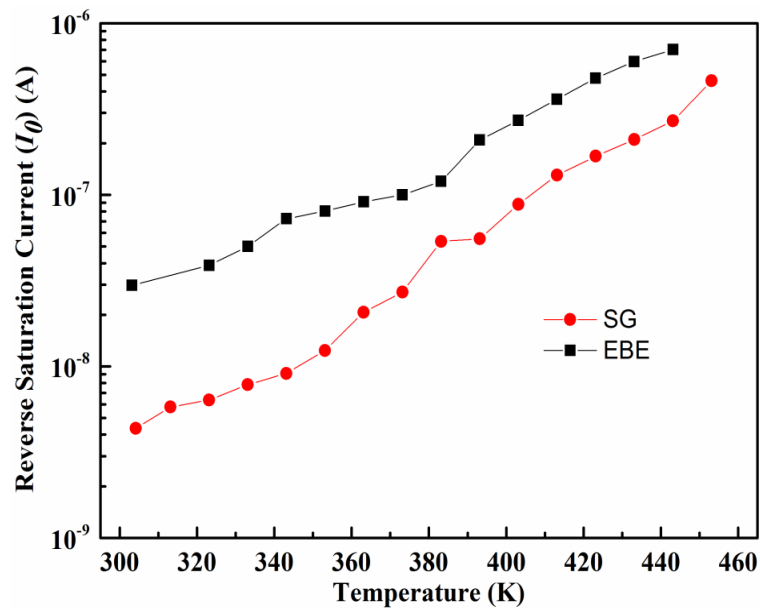


Figure 3.4: Variation of reverse saturation current (I_0) with temperature for both the devices fabricated using EBE and SG methods.

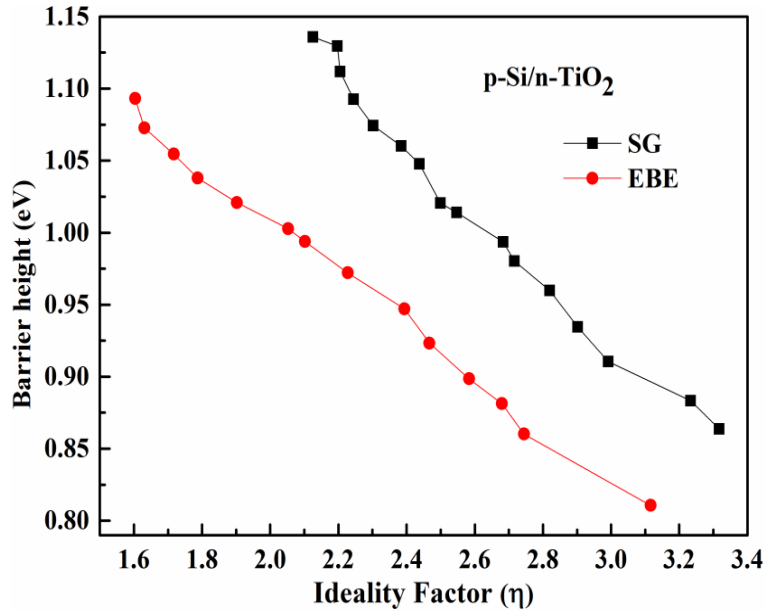


Figure 3.5: Variation of barrier height with ideality factor in the temperature range ~300 to 453 K for both devices fabricated using EBE and SG methods.

It is observed from Table 3.1 that the values of $I_0(T)$ and $\phi_{B,eff}$ are increased but η values are decreased with the increase in operating temperature. The change in $\phi_{B,eff}$ with temperature can be attributed to the BHI phenomenon commonly observed at the Schottky and heterojunction diodes as discussed earlier [Werner and Güttler (1991), Somvanshi and Jit (2013), Yadav *et al.* (2014), Hazra and Jit (2014-b), Somvanshi and Jit (2014)]. The BHI phenomenon demonstrates that barrier height at the p-Si/n-TiO₂ heterojunction is not constant as per Anderson model. Instead, it is a non-uniformly distributed random variable [Kroemer (1983), Werner and Güttler (1991)] due to non-ideal interface conditions. Since the kinetic energy of electrons is increased with temperature, the electrons can overcome higher barrier heights at higher temperatures thereby increasing the reverse saturation current and barrier height in the diode. This BHI phenomenon reduces the ideality factor (η) with increased temperatures [Werner and Güttler (1991), Yadav *et al.* (2014)]. The increasing values of barrier heights with respect to temperature confirms the existence of BHI at the interface [Chirakkara and

Krupanidhi (2012)]. In accordance with Tung's theoretical analysis [Tung (1992)] and experimental results of Schmitsdorf *et al.* [Somvanshi and Jit (2014)], the nearly linear relation between η and $\phi_{B,eff}$ as shown in Figure 3.5 confirms the existence of BHI for both types of n-TiO₂/p-Si heterojunction diodes under study.

3.3.2 Effect of Barrier Inhomogeneity on Temperature-Dependent Electrical Characteristics

In this section, we will estimate the temperature-dependent electrical parameters of the p-Si/n-TiO₂ heterojunctions under study by considering the BHI phenomenon. We will use the method proposed by Werner and Güttler (1991) [Werner and Güttler (1991)] where the non-uniform barrier height at the heterojunction interface is assumed to be a Gaussian distributed random variable.

3.3.3 Effect of BHI on the Richardson Constant

Non-ideal behavior of diode interface (n-TiO₂/p-Si) can be explained using Richardson plot shown in Figure 3.6. It is basically a plot of $\ln(I_0/T^2)$ versus q/kT . Using Eq. (3.2), it can be described as [Hazra and Jit (2014-b)]:

$$\ln\left(\frac{I_0}{T^2}\right) = \ln(AA^*) - \frac{q\phi_{B,eff}}{kT} \quad (3.6)$$

Note that we may get the values of Richardson constant and barrier height by the linear fitting of the Richardson plot for different temperatures ranging from 303 K to 354 K. The $\ln(I_0/T^2)$ vs. q/kT plot, named Richardson plot, is shown for both the diodes under study in Figure 3.6. As per Eq. (3.6), it is expected to have a linear relation between $\ln(I_0/T^2)$ and q/kT for ideal heterojunctions. However, the non-linear nature in Figure 3.6 again confirms the existence of BHI [Hazra and Jit (2014-b)] at the heterojunction

interface of the devices under study.

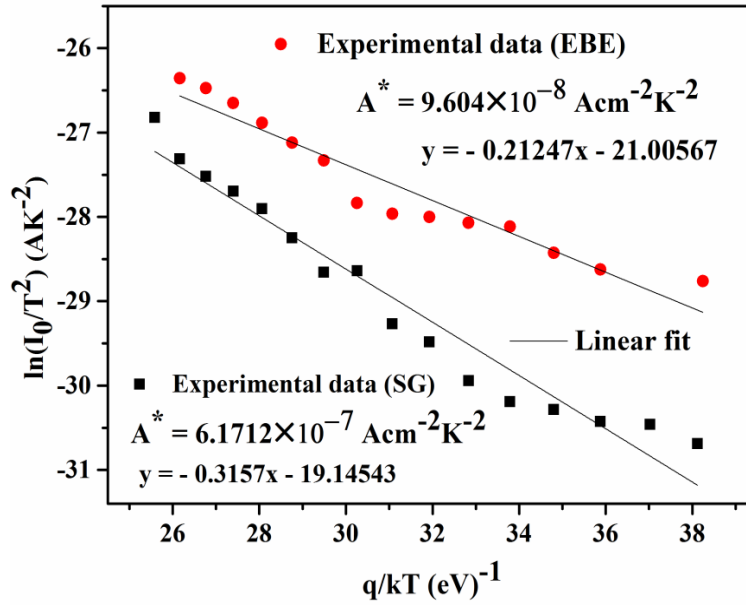


Figure 3.6: Typical $\ln(I_0/T^2)$ versus q/kT plot (i.e. Richardson plot) without taking the barrier inhomogeneity effects into consideration for both the devices fabricated using EBE and SG methods.

The intercept of linear-fit at the vertical axis in Figure 3.6 gives the value of Richardson's constant (A^*) as $\sim 9.604 \times 10^{-8} \text{ A cm}^{-2} \text{ K}^{-2}$ (for EBE device) and $\sim 6.1712 \times 10^{-7} \text{ A cm}^{-2} \text{ K}^{-2}$ (for SG device) without considering the BHI phenomenon. Clearly, both the estimated values are unrealistic values of Richardson's constant for n-TiO₂ against its theoretically predicated value of $\sim 1200 \text{ A cm}^{-2} \text{ K}^{-2}$ (for $m_n^* = 10m_o$) [Zhang *et al.* (2012-a)]. Also, from Figure 3.6, the estimated value of barrier height without consideration BHI is $\sim 0.212 \text{ eV}$ and $\sim 0.315 \text{ eV}$, respectively for the EBE and SG based diodes. We observe higher values of barrier height for SG based diode as compared to that of the EBE based diode. The significant difference between theoretical and experimental values of A^* is attributed to the BHI which is further discussed in the following subsections.

3.3.4 Determination of Mean Barrier Height and Modified Richardson Constant by Considering BHI Phenomenon

It is interesting to note that thermionic emission theory based I-V characteristics described by Eq. (3.1) assumes temperature-independent ideality factor and barrier height. However, the measured data shown in Table 3.1 demonstrate that both the parameters are highly temperature dependent due to the BHI phenomenon [Pakma *et al.* (2008-a)] at the p-Si/n-TiO₂ heterojunction interface as discussed earlier [Werner and Güttler (1991)].

Thus in this section, we will investigate the value of Richardson constant by including the BHI phenomenon. According to the model suggested by Werner and Güttler [Werner and Güttler (1991)], the barrier height is assumed as the Gaussian distributed random variable with a mean value ($\phi_{B0,m}$) and a standard deviation (σ_0). The probability density function, say $P(\phi_B)$, can be expressed as [Mtangi *et al.* (2009), Hazra and Jit (2014-b)]:

$$P(\phi_B) = \frac{1}{\sigma_S \sqrt{2\pi}} \exp\left[-\frac{(\phi_B - \phi_{B0,m})^2}{2\sigma_S^2}\right] \quad (3.7)$$

where, $\frac{1}{\sigma_S \sqrt{2\pi}}$ is the normalized constant, σ_0 is the standard deviation of mean barrier height ($\phi_{B0,m}$).

Following the methodology of Werner and Güttler [Werner and Güttler (1991)], the I-V-T model for the p-Si/n-TiO₂ can be described as:

$$I(V) = I_S \exp\left(\frac{qV}{\eta_{ap}(T)kT}\right) \times \left\{1 - \exp\left(-\frac{qV}{kT}\right)\right\} \quad (3.8)$$

where,

$$I_S = AA^*T^2 \exp\left(-\frac{q\phi_{ap}(T)}{kT}\right) \quad (3.9)$$

I_S is the modified reverse saturation current after incorporating BHI in the thermionic emission theory based current model described by Eq. (3.1). In addition, $\eta_{ap}(T)$ and $\phi_{ap}(T)$ denote the modified ideality factor and barrier height at zero bias which can be expressed as the functions of temperature. Now, the temperature dependent effective barrier height $\phi_{B,eff}(T)$ and ideality factor $\eta(T)$ can be expressed as [Werner and Güttler (1991), Mayimele *et al.* (2015)]:

$$\phi_{B,eff}(T) = \phi_{B0,m}(at T \approx 0) - (q\sigma_0^2/2kT) \quad (3.10)$$

$$(1/\eta(T) - 1) = \rho_1 - (q\rho_2/2kT) \quad (3.11)$$

$$\phi_{B,m}(V) = \phi_{B0,m} + \rho_1 V \quad (3.12)$$

$$\sigma^2(V) = \sigma_0^2 + \rho_2 V \quad (3.13)$$

where, ρ_1 and ρ_2 represent temperature-dependent voltage deformation coefficients of the barrier height distribution, $\phi_{B,m}(V)$ and $\sigma(V)$ are bias-dependent mean barrier height and standard deviation, respectively. It is important to note from Eq. (3.13) and Eq. (3.12) that standard deviation $\{\sigma(V)\}$ and mean barrier height $\{\phi_{B,m}(V)\}$ of Gaussian-distribution function are linearly-dependent on voltage (V). Notably subscript ‘0’ denotes thermodynamic equilibrium condition of the junction under study.

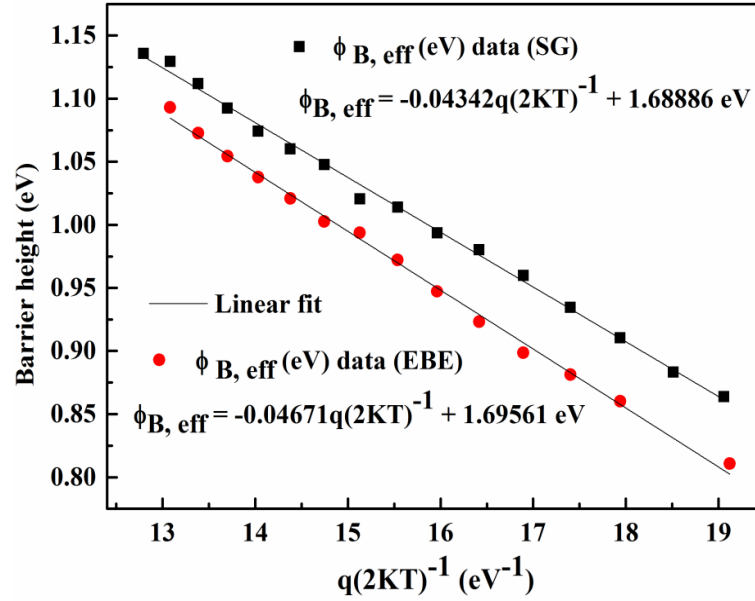


Figure 3.7: Barrier height $\{\phi_{B, \text{eff}}(T)\}$ variation with $q/2kT$ for both the devices fabricated using EBE and SG methods. The black straight line represents least-squares fit of the experimental data.

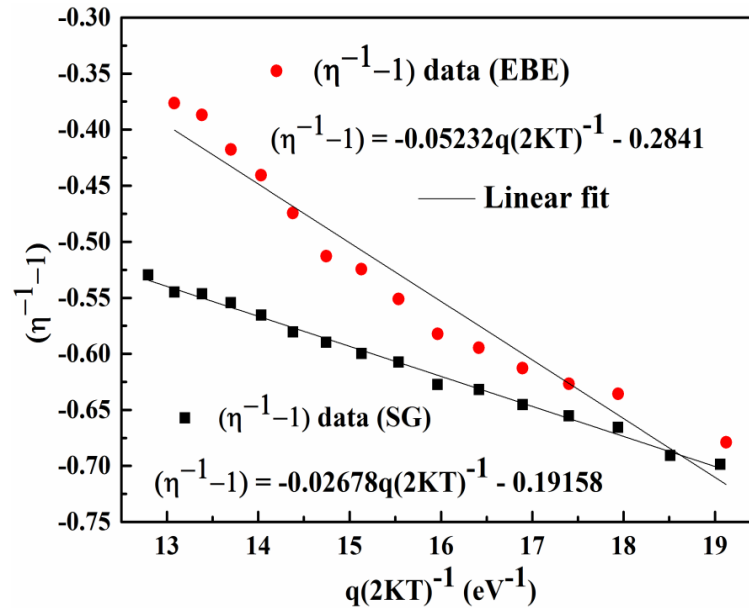


Figure 3.8: $(\eta^{-1}(T) - 1)$ variation with $q/2kT$ for both the devices fabricated using EBE and SG methods. The black straight line represents least-squares fit of the experimental data.

We now consider $\phi_{B,\text{eff}}(T)$ vs. $q/2kT$ and $(1/\eta(T)-1)$ vs. $q/2kT$ plots in Figure 3.7 and Figure 3.8, respectively. By using the respective least-squares linear fit approximation, we may obtain the following relations:

For the EBE based device:

$$\phi_{B,\text{eff}}(T) \approx 1.69561 - 0.04671 \times (q/2kT) \quad (3.14)$$

$$(1/\eta(T)-1) \approx -0.2841 - 0.05232 (q/2kT) \quad (3.15)$$

Similarly, for the SG based device:

$$\phi_{B,\text{eff}}(T) \approx 1.68886 - 0.04342 \times (q/2kT) \quad (3.16)$$

$$(1/\eta(T)-1) \approx -0.19158 - 0.02678 (q/2kT) \quad (3.17)$$

For the EBE based diode, comparing Eq. (3.10) and Eq. (3.14), we get $\phi_{B0,m} \approx 1.695$ eV and $\sigma_0 \approx 0.2161$ eV at 0 K. Similarly for the SG based diode, comparing Eq. (3.10) and Eq. (3.16), we get $\phi_{B0,m} \approx 1.688$ eV and $\sigma_0 \approx 0.2084$ eV at 0 K. The high value of σ_0 signifies less homogenous nature of barrier height and hence lower diode rectifying performance [Somvanshi and Jit (2013)]. Now for both the diodes under study, the mean barrier height at any specific temperature can be obtained from Eq. (3.10) by using its respective values of σ_0^2 and $\phi_{B0,m}(T=0)$. For example, at room temperature, the effective zero-bias mean barrier height i.e. $\phi_{B,\text{eff}}$ (at $T \sim 300$ K) ≈ 0.793 eV for EBE based diode and ≈ 0.849 eV for SG based diode which are very close to their theoretical values defined as the difference between work functions of Si and TiO₂ [Romero *et al.* (2004)]. Further, again for EBE based diode we may now compare Eq. (3.11) and Eq. (3.15) to obtain $\rho_1 \approx -0.2841$ V and $\rho_2 \approx -0.05232$ V. Similarly, for SG based diode we may now compare Eq. (3.11) and Eq. (3.17) to obtain $\rho_1 \approx -0.19158$ V and $\rho_2 \approx -0.02678$ V. Now, ρ_1 and ρ_2 of respective diodes can be used in Eq. (3.11) to

estimate the ideality factor at any desired temperature. Finally, using ρ_1 and ρ_2 in Eq. (3.12) and Eq. (3.13), respectively we can estimate the bias-dependent properties of mean barrier height and standard deviation.

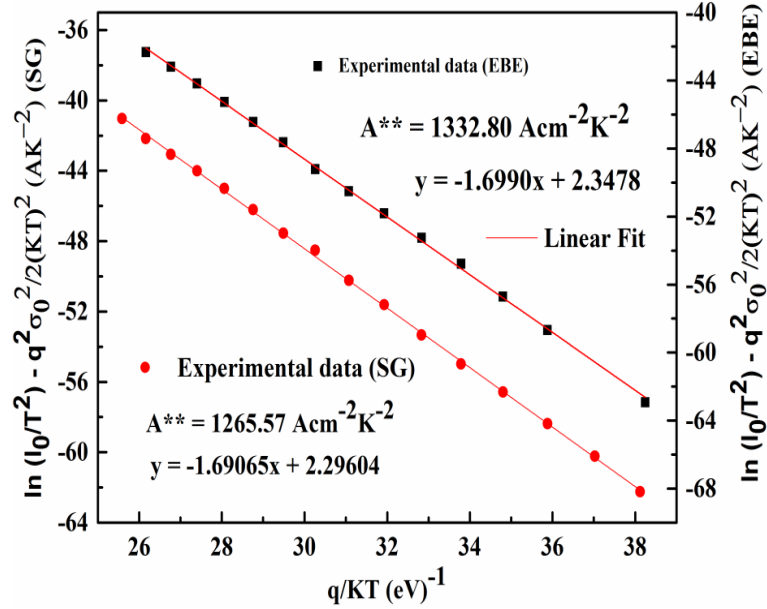


Figure 3.9: Modified Richardson plot (considering BHI) with its linear fit for p-Si/n-TiO₂ TF heterojunction diodes fabricated using EBE and SG methods.

To study the effect of BHI on the Richardson's constant (A^*), Eq. (3.10) can be used to modify Eq. (3.9) as [Somvanshi and Jit (2014), Mayimele *et al.* (2015)]:

$$\ln \left(\frac{I_0}{T^2} \right) - \left(\frac{q^2 \sigma_0^2}{2k^2 T^2} \right) = \ln (AA^{**}) - \frac{q \phi_{B0,m}(T=0)}{kT} \quad (3.18)$$

Now, the modified Richardson's plot is shown in Figure 3.9 for both the n-TiO₂/p-Si heterojunction diodes by taking BHI phenomenon into consideration. The linear fit intercept at the vertical axis is equated to $\ln (AA^{**})$ to obtain the estimated value of Modified Richardson constant (A^{**}). The estimated values of A^{**} for EBE and SG based diodes are $\sim 1332.80 \text{ Ac m}^{-2} \text{ K}^{-2}$ and $\sim 1265.57 \text{ Ac m}^{-2} \text{ K}^{-2}$, respectively. Thus, in contrary to the unrealistic values of $A^* \sim 9.604 \times 10^{-8} \text{ Ac m}^{-2} \text{ K}^{-2}$ for EBE based diode and A^*

$\sim 6.1712 \times 10^{-7} \text{ A cm}^{-2} \text{ K}^{-2}$ for SG based diode, the inclusion of BHI in the modified Richardson plot gives the values of the Richardson constants which are very close to the theoretically predicted value of $\sim 1200 \text{ A cm}^{-2} \text{ K}^{-2}$ [Zhang *et al.* (2012-a)] for TiO₂. Further, in case of EBE derived diode the value of barrier height $\sim 0.21 \text{ eV}$ as estimated from Figure 3.6 (without considering the BHI) is also significantly improved to $\phi_{B0,m}$ (at T $\sim 0 \text{ K}$) $\sim 1.688 \text{ eV}$ after taking the BHI phenomenon into consideration. Similarly, for the SG based diode, the value of barrier height of $\sim 0.31 \text{ eV}$ estimated from Figure 3.6 (without considering the BHI) is also significantly improved to $\phi_{B0,m}$ (at T $\sim 0 \text{ K}$) $\sim 1.69 \text{ eV}$ after taking the BHI phenomenon into consideration. The effective Richardson constants of EBE and SG derived TiO₂ TF have been estimated possibly for the first time from temperature-dependent current–voltage (I–V–T) characteristics of p-Si/n-TiO₂ TF heterojunction diode by including the Barrier Height Inhomogeneity (BHI).

3.4 Summary and Conclusion

In this chapter, the I-V-T characteristics of two n-TiO₂/p-Si heterojunction diodes fabricated in Chapter-2 have been analyzed in the operating temperature range of ~ 303 to 453 K for determining the temperature-dependent electrical parameters of the heterojunction diodes and the effective Richardson constant of n-TiO₂. The effects of the spatial Barrier Height Inhomogeneity (BHI) phenomenon on various temperature-dependent electrical parameters have been investigated by assuming a Gaussian distributed barrier height across the heterojunction interface. From the electrical measurements, we observe that the barrier height and ideality factor of the as-fabricated p-Si/n-TiO₂ devices are strong functions of the operating temperature. For EBE and SG

based diodes, the value of zero-bias mean barrier height ($\phi_{B0,m}$) (at $T \sim 0$ K) estimated from the Richardson's plot is increased from ~ 0.21 eV to ~ 1.68 eV and ~ 0.31 eV to ~ 1.69 eV, respectively, after taking the BHI effect into consideration. The value of Richardson constant is drastically improved from an unrealistic value of $\sim 9.604 \times 10^{-8} \text{ A cm}^{-2} \text{ K}^{-2}$ to $\sim 1332.80 \text{ A cm}^{-2} \text{ K}^{-2}$ for EBE based heterojunction and from $\sim 6.1712 \times 10^{-7} \text{ A cm}^{-2} \text{ K}^{-2}$ to $\sim 1265.57 \text{ A cm}^{-2} \text{ K}^{-2}$ for SG based heterojunction after taking BHI into consideration, which are very close to the theoretically predicted value of $\sim 1200 \text{ A cm}^{-2} \text{ K}^{-2}$ for TiO₂. The determination of Richardson constant from the I-V-T analysis of p-Si/n-TiO₂ is reported for the first time in this thesis.